

Short Note

Not peer-reviewed version

10-(3,5-Di-*tert*-butylphenyl)-9-Mesitylacridinium Tetrafluoroborate

[Yuki Itabashi](#) and [Kei Ohkubo](#)*

Posted Date: 6 March 2026

doi: 10.20944/preprints202603.0459.v1

Keywords: acridinium; acridinone; organic catalyst; grignard reaction; photoredox catalyst



Preprints.org is a free multidisciplinary platform providing preprint service that is dedicated to making early versions of research outputs permanently available and citable. Preprints posted at Preprints.org appear in Web of Science, Crossref, Google Scholar, Scilit, Europe PMC.

Copyright: This open access article is published under a [Creative Commons CC BY 4.0 license](#), which permit the free download, distribution, and reuse, provided that the author and preprint are cited in any reuse.

Disclaimer/Publisher's Note: The statements, opinions, and data contained in all publications are solely those of the individual author(s) and contributor(s) and not of MDPI and/or the editor(s). MDPI and/or the editor(s) disclaim responsibility for any injury to people or property resulting from any ideas, methods, instructions, or products referred to in the content.

Short Note

10-(3,5-Di-*tert*-butylphenyl)-9-Mesitylacridinium Tetrafluoroborate

Yuki Itabashi ¹ and Kei Ohkubo ^{1,2,*}

¹ Institute for Open and Transdisciplinary Research Initiatives (OTRI), The University of Osaka, 1-6 Yamada-oka, Suita, Osaka 565-0871, Japan

² Organization for Carbon Neutrality Collaboration (OCNC), The University of Osaka, 1-6 Yamada-oka, Suita, Osaka 565-0871, Japan

* Correspondence: ohkubo@irdd.osaka-u.ac.jp

Abstract

9-Mesitylacridinium salts are widely recognized as efficient organic photoredox catalysts owing to their strong excited-state oxidizing power and stability under visible-light irradiation. In this study, a new mesityl acridinium derivative bearing a di-*tert*-butylphenyl substituent on the nitrogen atom was synthesized. The introduction of *tert*-butyl groups on the *N*-aryl moiety was primarily aimed at improving solubility and chemical stability of the acridinium salt. The target compound was obtained in high overall yield starting from a 9(10*H*)-acridinone precursor through a concise synthetic sequence. The synthesis consists of a copper-catalyzed C–N coupling reaction to install the aryl substituent on the nitrogen atom, followed by a Grignard reaction and subsequent acid treatment to afford the corresponding acridinium salt. All transformations proceeded smoothly, providing efficient access to the desired novel acridinium derivative. This work presents a practical example of structural modification of mesitylacridinium derivatives directed toward enhanced solubility and stability, and provides a useful synthetic platform for the preparation of structurally diverse acridinium salts.

Keywords: acridinium; acridinone; organic catalyst; grignard reaction; photoredox catalyst

1. Introduction

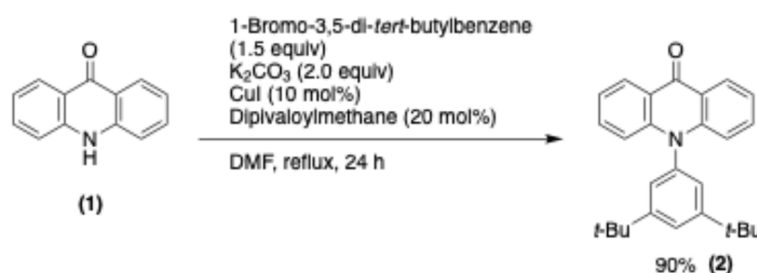
Organic photoredox catalysis has emerged as a powerful strategy for promoting synthetically valuable transformations under mild reaction conditions, enabling access to reactive radical intermediates with high chemoselectivity and functional group tolerance [1–6]. Among the diverse classes of organic photocatalysts, acridinium salts have attracted sustained attention owing to their exceptionally efficient photoredox ability and modular structural tunability [7–11]. In particular, 9-mesityl-substituted acridinium catalysts, exemplified by *N*-methyl mesityl acridinium, display a nearly orthogonal arrangement between the acridinium core and the mesityl substituent [12]. Upon photoexcitation of the acridinium chromophore, rapid intramolecular electron transfer from the mesityl donor to the acridinium acceptor generates a long-lived charge-separated state [12,13]. This unique donor–acceptor electronic architecture suppresses rapid back-electron transfer and endows the catalyst with remarkable oxidative power in the excited state. As a consequence, mesitylacridinium derivatives have been extensively developed and applied to a wide range of oxidative C–H functionalizations, dehydrogenative couplings, and atom-transfer processes [14–21].

Despite these advances, structural variation at the nitrogen position has remained comparatively less explored, particularly with sterically demanding aryl substituents. We envisioned that incorporation of an aryl group bearing two *tert*-butyl substituents at the nitrogen atom would provide additional steric protection and increase solubility in organic media, especially in systems involving π -extension or multiple aryl substitutions on the acridinium framework. Guided by this design

concept, we report herein the synthesis of 10-(3,5-di-*tert*-butylphenyl)-9-mesitylacridinium tetrafluoroborate as a novel *N*-aryl-substituted mesitylacridinium derivative.

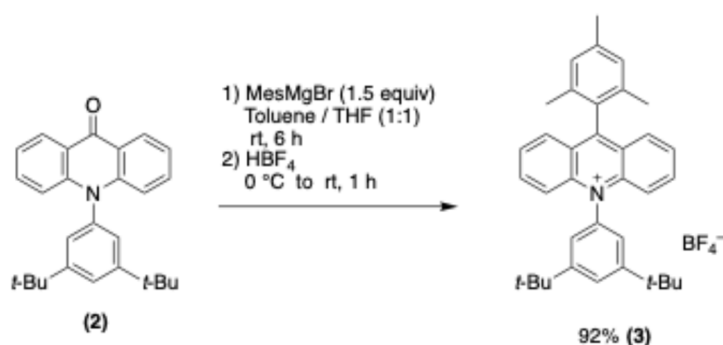
2. Results and Discussion

Commercially available 9(10*H*)-acridinone (1) was selected as the starting material, and *N*-arylation was accomplished via an Ullmann–Goldberg coupling strategy (Scheme 1) [22–27]. The aryl group was introduced using 1-bromo-3,5-di-*tert*-butylbenzene as the coupling partner in the presence of CuI and a β -diketone ligand, dipivaloylmethane [28], which is well established to promote efficient C–N bond formation under Ullmann–Goldberg coupling conditions. The reaction proceeded smoothly in DMF with potassium carbonate as the base under an inert atmosphere, delivering the desired *N*-aryl 9(10*H*)-acridinone in high yield. After aqueous workup and purification, 10-(3,5-di-*tert*-butylphenyl)-9(10*H*)-acridinone (2) was obtained as a pale yellow solid in 90% yield.



Scheme 1. Ullmann–Goldberg coupling reaction for *N*-arylation.

9-Mesityl substitution was introduced by a Grignard reaction followed by acid treatment of 10-(3,5-di-*tert*-butylphenyl)-9(10*H*)-acridinone (2) (Scheme 2). To a solution of 10-(3,5-di-*tert*-butylphenyl)-9(10*H*)-acridinone (2) in toluene was slowly added, via syringe, a separately prepared ca. 1.0 M THF solution of mesitylmagnesium bromide (MesMgBr, 1.5 equiv). During the addition, the reaction mixture gradually turned red. After stirring at room temperature for 6 h, the reaction mixture was cooled to 0 °C using an ice–water bath, and an excess amount of 48 wt% aqueous tetrafluoroboric acid (HBF₄) was added, resulting in a color change to yellow.



Scheme 2. Grignard reaction for mesityl substitution.

The mixture was extracted with chloroform, and NaBF₄ was added to remove residual water from the organic phase. After filtration and concentration, the residue was dissolved in a small amount of dichloromethane, and diethyl ether was slowly added dropwise with stirring. A yellow precipitate formed, and diethyl ether was further added until no additional precipitate was observed. The resulting solid was collected by filtration to afford 10-(3,5-di-*tert*-butylphenyl)-9-mesitylacridinium tetrafluoroborate (3) as a yellow solid in 92% yield.

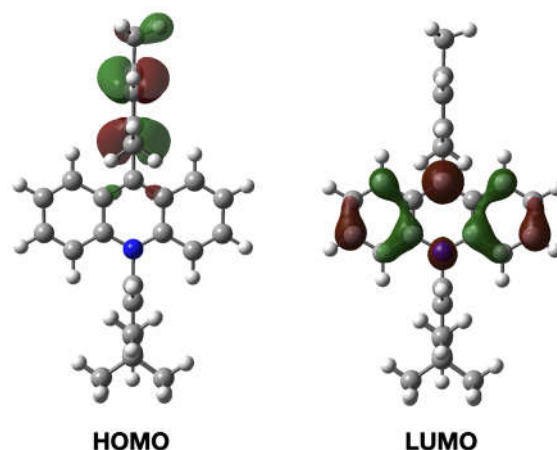


Figure 1. Kohn–Sham HOMO and LUMO of **3** obtained from DFT calculations. Isosurfaces are plotted at 0.04 a.u.

Computational studies were conducted at the CAM-B3LYP/6-311+G(d,p) level of theory to elucidate the electronic structure of the acridinium derivative. Geometry optimization revealed that the acridinium core and the mesityl substituent at the 9-position adopt an almost perfectly orthogonal conformation, with a calculated dihedral angle of 89.86° , effectively suppressing π -conjugative interaction between the two π -systems. This geometric decoupling is directly reflected in the Kohn–Sham frontier molecular orbitals: the HOMO is predominantly localized on the mesityl moiety, whereas the LUMO is primarily distributed over the acridinium framework. The corresponding orbital energies were calculated to be -5.12 eV (HOMO) and -10.67 eV (LUMO). Notably, this pronounced spatial separation of the frontier orbitals, together with the associated energy alignment, closely parallels the electronic structure reported for 10-methyl-9-mesitylacridinium, a prototypical organic photoredox catalyst. These results demonstrate that the present system preserves the characteristic donor–acceptor electronic architecture underlying efficient photoredox reactivity.

3. Materials and Methods

3.1. Materials

9(10*H*)-Acridinone (**1**), 1-bromo-3,5-di-*tert*-butylbenzene, and mesityl bromide were purchased from TCI (Tokyo, Japan). 48 wt% aqueous tetrafluoroboric acid was purchased from Sigma-Aldrich Co. LLC (St. Louis, MO, USA). All the other reagents were commercially available (reagent grade from TCI (Tokyo, Japan), FUJIFILM Wako Pure Chemical Corporation (Osaka, Japan), KISHIDA Chemical Co., Ltd. (Osaka, Japan), Kanto Chemical Co., Inc. (Tokyo, Japan), and Sigma-Aldrich Co. LLC (St. Louis, MO, USA)) and used as received. Flash column chromatography was performed with 40–50 mm Silica Gel 60 N (Kanto Chemical Co., Inc.). Nuclear magnetic resonance (NMR) spectra were recorded using a JEOL JMN-ECS-400 (^1H : 400 MHz, ^{13}C : 100 MHz) (Tokyo, Japan), with chemical shifts calibrated using tetramethylsilane (0 ppm for ^1H NMR) or residual undeuterated solvent (CHCl_3 at 77.16 ppm for ^{13}C NMR). The abbreviations for multiplicities are as follows: s (singlet), d (doublet), t (triplet), q (quartet), m (multiplet), and br (broad). High-resolution mass spectra were acquired with a JEOL JMS-T100LP (Tokyo, Japan).

3.2. Synthetic Procedures

A flame-dried Schlenk tube equipped with a magnetic stir bar was charged with 9(10*H*)-acridinone (**1**, 390 mg, 2.0 mmol), CuI (38 mg, 0.20 mmol, 10 mol %), K_2CO_3 (553 mg, 4.0 mmol, 2.0 equiv), and 1-bromo-3,5-di-*tert*-butylbenzene (808 mg, 3.0 mmol, 1.5 equiv). The tube was evacuated and backfilled with argon (three cycles). Dipivaloylmethane (74 mg, 0.40 mmol, 20 mol %, 82 μL) and

DMF (2 mL) were then added under an argon atmosphere. The reaction mixture was heated at reflux with stirring for 24 h.

After cooling to room temperature, an aqueous solution of NH_4Cl was added, and the mixture was stirred for 1 h. The reaction mixture was diluted with CHCl_3 and transferred to a separatory funnel. The organic layer was separated, washed with brine, dried over anhydrous Na_2SO_4 , filtered, and concentrated under reduced pressure. Reprecipitation from $\text{CHCl}_3/\text{MeOH}$ afforded the crude solid, which was collected by filtration and dried under vacuum to give 10-(3,5-di-*tert*-butylphenyl)-9(10*H*)-acridinone (**2**) as a pale yellow solid (690 mg, 90%). $^1\text{H-NMR}$ (400 MHz, chloroform-*d*) δ 8.61 (dd, $J = 8.0, 1.6$ Hz, 2H), 7.67 (t, $J = 1.8$ Hz, 1H), 7.54-7.50 (m, 2H), 7.31-7.29 (m, 2H), 7.17 (d, $J = 1.8$ Hz, 2H), 6.78 (d, $J = 8.2$ Hz, 2H), 1.38 (s, 18H). The spectrum is shown in Figure S1.

A flame-dried Schlenk tube equipped with a magnetic stir bar was charged with 10-(3,5-di-*tert*-butylphenyl)-9(10*H*)-acridinone (**2**, 384 mg, 1.0 mmol) under an argon atmosphere. Toluene (1.5 mL) was added, and the resulting suspension was stirred. A 1.0 M solution of mesitylmagnesium bromide in THF (1.5 mL, 1.5 mmol, 1.5 equiv), prepared from mesityl bromide and magnesium, was added dropwise at room temperature. The reaction mixture was stirred for 6 h at room temperature. The reaction was then cooled in an ice-water bath, and 48 wt% aqueous tetrafluoroboric acid (1.0 mL) was added slowly dropwise with stirring. After stirring for 1 hour at 0 °C to room temperature, water and CHCl_3 were added, and the layers were separated. The organic phase was treated with NaBF_4 to remove residual water, filtered, and concentrated under reduced pressure. Reprecipitation from $\text{CH}_2\text{Cl}_2/\text{diethyl ether}$ afforded 10-(3,5-di-*tert*-butylphenyl)-9-mesitylacridinium tetrafluoroborate (**3**) as a yellow solid (448 mg, 92%). $^1\text{H-NMR}$ (400 MHz, chloroform-*d*) δ 8.17 (ddd, $J = 9.2, 6.9, 1.4$ Hz, 2H), 7.93 (dd, $J = 8.7, 0.9$ Hz, 2H), 7.89 (t, $J = 1.6$ Hz, 1H), 7.81 (ddd, $J = 8.7, 6.9, 0.9$ Hz, 2H), 7.60 (d, $J = 9.2$ Hz, 2H), 7.51 (d, $J = 1.4$ Hz, 2H), 7.18 (s, 2H), 2.50 (s, 3H), 1.87 (s, 6H), 1.44 (s, 18H). The spectrum is shown in Figure S2. $^{13}\text{C}\{^1\text{H}\}\text{-NMR}$ (101 MHz, chloroform-*d*) δ 164.3, 155.3, 142.2, 140.5, 139.0, 136.8, 136.4, 129.4, 129.2, 128.9, 128.7, 126.2, 125.6, 122.2, 120.3, 35.7, 31.5, 21.4, 20.3. The spectrum is shown in Figure S3. HRMS (ESI) m/z ($[\text{M}]^+$) calcd for $\text{C}_{36}\text{H}_{40}\text{N}$: 486.31553, found: 486.31518. The spectrum is shown in Figure S4. FT-IR (ATR) ν_{max} (cm^{-1}): 2957, 2884, 1607, 1577, 1539, 1463, 1436, 1384, 1362, 1048, 1033. The spectrum is shown in Figure S5.

3.3. Calculations

DFT calculations were carried out with Gaussian 16 (Revision C.02, Gaussian, Inc., Wallingford, CT, USA) [29]. Geometry optimization for ground-state species was performed using the CAM-B3LYP functional [30] in combination with the 6-311+G(d,p) basis set. Vibrational frequency analysis was conducted at the same level of theory to characterize each stationary point: minimum was confirmed to have no imaginary frequencies. Cartesian coordinate of the optimized structure is shown in Table 1.

4. Conclusions

In summary, we have designed and synthesized 10-(3,5-di-*tert*-butylphenyl)-9-mesitylacridinium tetrafluoroborate (**3**) through sequential *N*-arylation of 9(10*H*)-acridinone (**1**) followed by mesityl Grignard addition and acid-mediated cyclization. The target acridinium salt was obtained in high overall yield under operationally straightforward conditions. Computational analysis at the CAM-B3LYP/6-311+G(d,p) level revealed an almost perfectly orthogonal arrangement between the acridinium core and the mesityl substituent (dihedral angle = 89.86°), leading to pronounced spatial separation of the Kohn–Sham frontier orbitals. The HOMO–LUMO distribution and energy profile closely parallel those of established mesitylacridinium systems, indicating preservation of the characteristic donor–acceptor electronic architecture. The present study provides a new *N*-aryl-substituted mesitylacridinium framework and contributes to the structural diversification of acridinium-based photocatalysts.

Supplementary Materials: The following supporting information can be downloaded at the website of this paper posted on Preprints.org, Figure S1-S3: ^1H and ^{13}C NMR spectra; Figure S4-S5, MS and IR spectra; Table S1: cartesian coordinate.

Author Contributions: Conceptualization, Y.I., and K.O.; methodology, Y.I., and K.O.; validation, Y.I., and K.O.; formal analysis, Y.I.; investigation, Y.I.; resources, K.O.; writing—review and editing, Y.I., and K.O.; supervision, Y.I., and K.O. All authors have read and agreed to the published version of the manuscript.

Funding: This work was supported by JSPS KAKENHI Grants (JP23K13709 to Y.I., and JP24K21770 to K.O.).

Data Availability Statement: The Supplementary Materials are available free of charge on the website.

Acknowledgments: The authors thank the Faculty of Pharmaceutical Sciences, The University of Osaka, for assistance with high-resolution mass spectrometry (HRMS) measurements. The authors also thank Ms. Kei Umino for assistance with the synthesis.

Conflicts of Interest: The authors declare no conflicts of interest.

References

1. Fukuzumi, S.; Ohkubo, K. Organic Synthetic Transformations using Organic Dyes as Photoredox Catalysts. *Org. Biomol. Chem.* **2014**, *12*, 6059–6071.
2. Fukuzumi, S.; Ohkubo, K. Selective Photocatalytic Reactions with Organic Photocatalysts. *Chem. Sci.* **2013**, *4*, 561–574.
3. Shaw, M.H.; Twilton, J.; MacMillan, D.W.C. Photoredox Catalysis in Organic Chemistry. *J. Org. Chem.* **2016**, *81*, 6898–6926.
4. Fukuzumi, S.; Lee, Y.-M.; Nam, W. Bioinspired artificial photosynthesis systems. *Tetrahedron* **2020**, *76*, 131024
5. Lee, Y.-M.; Nam, W.; Fukuzumi, S. Redox catalysis via photoinduced electron transfer. *Chem. Sci.* **2023**, *14*, 4205–4218
6. Yoshimi, Y. Organic Photoredox Reactions in Two-Molecule Photoredox System. *Chem. Rec.* **2024**, *24*, e202300326.
7. Fukuzumi, S.; Kuroda, S.; Tanaka, T. Selective Photoalkylation of 10-Methylacridinium Ion with Tetraalkylstannanes or Diethylmercury Using Visible Irradiation. *J. Chem. Soc., Chem. Commun.* **1986**, 1553–1554.
8. Fukuzumi, S.; Kuroda, S.; Tanaka, T. Substrate-Selective Photo-Oxidation of Benzyl Alcohol Derivatives with Oxygen, Catalysed by an NAD^+ Model Compound. *J. Chem. Soc., Chem. Commun.* **1987**, 120–122.
9. Fukuzumi, S.; Kitano, T.; Tanaka, T. Reduction of 10-Methylacridinium Ion with Fatty Acids by Photoinduced Electron-Transfer Reactions. *Chem. Lett.* **1989**, *18*, 1231–1234.
10. Fukuzumi, S.; Kitano, T.; Mochida, K. Photo-Induced One-Electron Reduction of 10-Methylacridinium Ion with Group 14 Dimetallic Compounds Using Visible Irradiation. *J. Chem. Soc., Chem. Commun.* **1990**, 1236–1237.
11. Fukuzumi, S.; Yorisue, T. 10,10'-Dimethyl-9,9'-biacridine Acting as a Unique Electron Source Compared with the Corresponding Monomer for the Efficient Reduction of Dioxygen, Catalysed by a Cobalt Porphyrin in the Presence of Perchloric Acid. *J. Chem. Soc., Perkin Trans. 2* **1991**, 1607–1611.
12. Fukuzumi, S.; Kotani, H.; Ohkubo, K.; Ogo, S.; Tkachenko, N.V.; Lemmetyinen, H. Electron-Transfer State of 9-Mesityl-10-methylacridinium Ion with a Much Longer Lifetime and Higher Energy Than That of the Natural Photosynthetic Reaction Center. *J. Am. Chem. Soc.* **2004**, *126*, 1600–1601.
13. Hoshino, M.; Uekusa, H.; Tomita, A.; Koshihara, S.; Sato, T.; Nozawa, S.; Adachi, S.; Ohkubo, K.; Kotani, H.; Fukuzumi, S. Determination of the Structural Features of a Long-Lived Electron-Transfer State of 9-Mesityl-10-methylacridinium Ion. *J. Am. Chem. Soc.* **2012**, *134*, 4569–4572.
14. Ohkubo, K.; Fujimoto, A.; Fukuzumi, S. Metal-free Oxygenation of Cyclohexane with Oxygen Catalyzed by 9-Mesityl-10-methylacridinium and Hydrogen Chloride under Visible Light Irradiation. *Chem. Commun.* **2011**, *47*, 8515–8517.

15. Joshi-Pangu, A.; Lévesque, F.; Roth, H.G.; Oliver, S.F.; Campeau, L.-C.; Nicewicz, D.; DiRocco, D.A. Acridinium-Based Photocatalysts: A Sustainable Option in Photoredox Catalysis. *J. Org. Chem.* **2016**, *81*, 7244–7249.
16. White, A.R.; Wang, L.; Nicewicz, D.A. Synthesis and Characterization of Acridinium Dyes for Photoredox Catalysis. *Synlett* **2019**, *30*, 827–832.
17. Lakhdar, S. Acridinium Salts and Cyanoarenes as Powerful Photocatalysts: Opportunities in Organic Synthesis. *Chem. Rev.* **2021**, *121*, 19526–19549.
18. Itabashi, Y.; Asahara, H.; Ohkubo, K. Chlorine-Radical-Mediated C–H Oxygenation Reaction under Light Irradiation. *Chem. Commun.* **2023**, *59*, 7506–7517.
19. Tanabe, S.; Mitsunuma, H.; Kanai, M. Catalytic Allylation of Aldehydes Using Unactivated Alkenes. *J. Am. Chem. Soc.* **2020**, *142*, 12374–12381.
20. Matsuda, M.; Uchiyama, M.; Itabashi, Y.; Ohkubo, K.; Kamigaito, M. Acridinium Salts as Photoredox Organocatalysts for Photomediated Cationic RAFT and DT Polymerizations of Vinyl Ethers. *Polym. Chem.* **2022**, *13*, 1031–1039.
21. Ohkubo, K.; Matsumoto, S.; Asahara, H.; Fukuzumi, S. 9-(4-Halo-2,6-xylyl)-10-methylacridinium Ion as an Effective Photoredox Catalyst for Oxygenation and Trifluoromethylation of Toluene Derivatives. *ACS Catal.* **2024**, *14*, 2671–2684.
22. Ullmann, F. Ueber eine neue Bildungsweise von Diphenylaminderivaten. *Ber. Dtsch. Chem. Ges.* **1903**, *36*, 2382–2384.
23. Ullmann, F. Ueber eine neue Darstellungsweise von Phenyläthersalicylsäure. *Ber. Dtsch. Chem. Ges.* **1904**, *37*, 853–854.
24. Goldberg, I. Ueber Phenylirungen bei Gegenwart von Kupfer als Katalysator. *Ber. Dtsch. Chem. Ges.* **1906**, *39*, 1691–1692.
25. Ley, S. V.; Thomas, A. W. Modern Synthetic Methods for Copper-Mediated C(aryl)–O, C(aryl)–N, and C(aryl)–S Bond Formation. *Angew. Chem. Int. Ed.* **2003**, *42*, 5400–5449.
26. Kunz, K.; Scholz, U.; Ganzer, D. Renaissance of Ullmann and Goldberg Reactions—Progress in Copper-Catalyzed C–N-, C–O-, and C–S-Coupling. *Synlett* **2003**, *15*, 2428–2439.
27. Seifinoferest, B.; Tanbakouchian, A.; Larijani, B.; Mahdavi, M. Ullmann–Goldberg and Buchwald–Hartwig C–N Cross Couplings: Synthetic Methods to Pharmaceutically Potential N-Heterocycles. *Asian J. Org. Chem.* **2021**, *10*, 1319–1344.
28. Buck, E.; Song, Z. J.; Tschäen, D.; Dormer, P. G.; Volante, R. P.; Reider, P. J. Ullmann Diaryl Ether Synthesis: Rate Acceleration by 2,2,6,6-Tetramethylheptane-3,5-dione. *Org. Lett.* **2002**, *4*, 1623–1626.
29. Gaussian 16, Revision C.02, M. J. Frisch, G. W. Trucks, H. B. Schlegel, G. E. Scuseria, M. A. Robb, J. R. Cheeseman, G. Scalmani, V. Barone, G. A. Petersson, H. Nakatsuji, X. Li, M. Caricato, A. V. Marenich, J. Bloino, B. G. Janesko, R. Gomperts, B. Mennucci, H. P. Hratchian, J. V. Ortiz, A. F. Izmaylov, J. L. Sonnenberg, D. Williams-Young, F. Ding, F. Lipparini, F. Egidi, J. Goings, B. Peng, A. Petrone, T. Henderson, D. Ranasinghe, V. G. Zakrzewski, J. Gao, N. Rega, G. Zheng, W. Liang, M. Hada, M. Ehara, K. Toyota, R. Fukuda, J. Hasegawa, M. Ishida, T. Nakajima, Y. Honda, O. Kitao, H. Nakai, T. Vreven, K. Throssell, J. A. Montgomery, Jr., J. E. Peralta, F. Ogliaro, M. J. Bearpark, J. J. Heyd, E. N. Brothers, K. N. Kudin, V. N. Staroverov, T. A. Keith, R. Kobayashi, J. Normand, K. Raghavachari, A. P. Rendell, J. C. Burant, S. S. Iyengar, J. Tomasi, M. Cossi, J. M. Millam, M. Klene, C. Adamo, R. Cammi, J. W. Ochterski, R. L. Martin, K. Morokuma, O. Farkas, J. B. Foresman, D. J. Fox, Gaussian, Inc. Wallingford CT, **2019**.
30. Yanai, T.; Tew, D.; Handy, N. A new hybrid exchange-correlation functional using the Coulomb-attenuating method (CAM-B3LYP). *Chem. Phys. Lett.* **2004**, *393*, 51–57.

Disclaimer/Publisher's Note: The statements, opinions and data contained in all publications are solely those of the individual author(s) and contributor(s) and not of MDPI and/or the editor(s). MDPI and/or the editor(s) disclaim responsibility for any injury to people or property resulting from any ideas, methods, instructions or products referred to in the content.